



Observer-based finite-time adaptive neural network control for PMSM with state constraints

Sihui Zhou¹ · Shuai Sui¹ · Yongming Li¹ · Shaocheng Tong¹

Received: 17 August 2022 / Accepted: 7 November 2022 / Published online: 24 November 2022
© The Author(s), under exclusive licence to Springer-Verlag London Ltd., part of Springer Nature 2022

Abstract

This article investigates the observer-based finite-time adaptive neural network control for the permanent magnet synchronous motor (PMSM) system. The addressed PMSM system includes unknown nonlinear dynamics and constraint immeasurable states. The neural networks are utilized to approximate the unknown nonlinear dynamics and an equivalent control design model is established, by which a neural network state observer is given to estimate the immeasurable states. By constructing barrier Lyapunov functions and under the framework of adaptive backstepping control design technique and finite-time stability theory, a finite-time adaptive neural network control scheme is developed. It is proved that the proposed control scheme ensures the closed-loop system stable and the angular velocity, stator current and other state variables not to exceed their predefined bounds in a finite time. Finally, the computer simulation and a comparison with the existing controller are provided to confirm the effectiveness of the presented controller.

Keywords Permanent magnet synchronous motor system · Full-state constraints · Adaptive neural networks output-feedback control · Finite-time control and stability

1 Introduction

Over the past decades, the demand for PMSMs is growing in numerous industrial equipment fields including vehicles, machine tools, and robots [1–4]. Nevertheless, PMSM systems are nonlinear, multivariable and strongly coupled objects, which usually face model uncertainties caused by parameter variations and unavoidable external disturbances in industrial applications. Therefore, to solve the above difficulties and achieve the higher requirements of PMSMs in practical application, some effective control methods are proposed for PMSM systems, such as backstepping

controllers [5], adaptive controllers [6], sliding mode controllers [7] and disturbance rejection control [8].

In the practical engineering, since the considered PMSM systems are often complex and uncertainties, they are difficult to model accurately. To handle this problem, some intelligent adaptive control methods including neural network controllers and fuzzy controllers have been widely adopted in the control of PMSMs [9–16]. In [9–13], some adaptive fuzzy control methods were presented for position tracking control of PMSMs via backstepping design technique. The authors in [14] proposed a robust adaptive fuzzy controller by dead-zone smooth inverse compensation scheme for PMSMs. In addition, the violations of the state constraints often result in system instability, performance degradation, or even system damage. Thus, the researching state constraint control problem is very significant for PMSM systems [15, 16]. In [15], the authors used the barrier Lyapunov function and proposed an output constraint control method of the PMSM system. Furthermore, the adaptive neural network control scheme [16] was designed for the PMSM system with full state constraints.

It should be mentioned that the aforementioned control strategies are developed by the asymptotic stability theory.

✉ Shaocheng Tong
tongshaocheng@lnut.edu.cn

Sihui Zhou
zhoush0601@163.com

Shuai Sui
shuaisui2011@163.com

Yongming Li
l_y_m_2004@163.com

¹ College of Science, Liaoning University of Technology, Shiying, Jinzhou 121001, Liaoning, China

Hence, they only guarantee the controller systems are stable in infinite time. In fact, there are many practical systems like the PMSM system addressed in this study, they are more desired that the state trajectories converge to the stable equilibrium point within a finite-time interval rather than an infinite time. For this purpose, the finite-time stability is proposed by [17]. Since the finite-time stability has the properties such as fast transient and better robustness against the uncertainties. Thus, by the finite-time stability theory, many finite-time control methods for PMSMs have been developed during the past few years [18–22]. The literature [18] developed a neural networks finite-time adaptive dynamic surface control method for PMSMs. By combining backstepping control technology with the command filtered technology, [19] studied the fuzzy finite time tracking control problem for PMSMs. [20] considered the finite-time neural network position tracking control scheme considered for the fractional-order chaotic permanent magnet synchronous motor system. In [21, 22], the adaptive finite-time neural network control schemes were proposed for uncertain permanent magnet synchronous motor system. However, to the best of authors' knowledge, there are few results on finite-time output feedback control for the PMSMs with full state constraints, which prompts us to conduct this study. Note that when the states are not measurable, the state observer becomes an extremely effective technique to solve the state immeasurable problem. In [23–26], the output feedback controllers were applied to control PMSMs with state immeasurable. However, the state observers were designed in [23–26] all focus on the PMSM systems whose the nonlinear dynamics are required to be known. Nevertheless, the output-feedback controllers are designed by the asymptotic stability theory and without considering the state constraint control problem.

Based on the above observations, this paper investigates the finite-time neural adaptive output feedback tracking control problem for PMSM system. The considered PMSM system contains unknown nonlinear dynamics and constraint immeasurable states. The neural networks are utilized to approximate the unknown nonlinear dynamics, a neural network state observer is designed to estimate the immeasurable states. By constructing barrier Lyapunov functions and under the framework of adaptive backstepping control design technique and finite-time stability theory, a finite-time adaptive neural network control scheme is developed. The main advantages of the proposed output-feedback control approach are as follows.

- (i) This paper proposes an observer-based finite-time adaptive output feedback control method for the PMSM system via a novel neural network state observer. Note that the previous finite-time fuzzy or neural network control schemes [7, 8, 25] all require that the angular velocity, stator current and other state variables of the PMSM system must be measurable. Thus, they can not solve the state immeasurable problem addressed by this study.
- (ii) The proposed the observer-based neural network adaptive output feedback controller is designed under the finite-time stability theory. Therefore, it not only can ensure the closed-loop system stable, but also guarantee the angular velocity, stator current and other state variables not exceed their predefined bounds in a finite time. More importantly, it has fast convergence and better robustness to the uncertainties compared with the previous output feedback controllers [15] developed under the asymptotic stability.

2 System description and some preliminaries

2.1 System description

The d - q -axis stator voltage model of PMSMs considered in this paper is shown by Fig. 1. The mathematical equations of PMSMs are expressed by

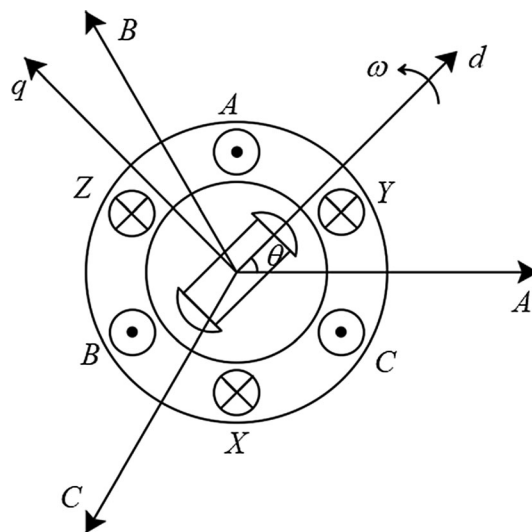


Fig. 1 Structure of the considered PMSM system

$$\begin{aligned}
 J \frac{d\omega}{dt} &= \frac{3}{2} n_p [(L_d - L_q) i_d i_q + \Phi i_q] - T_L - B\omega \\
 L_d \frac{di_d}{dt} &= -R_s i_d + n_p \omega L_q i_q + u_d \\
 L_q \frac{di_q}{dt} &= -R_s i_q - n_p \omega L_d i_d + u_q - n_p \omega \Phi \\
 \frac{d\theta}{dt} &= \omega
 \end{aligned}
 \tag{1}$$

In (1), u_q and u_d express system control inputs, i_q, i_d, θ and ω are the system state variables, they are d - q -axis current, and the rotor position and motor rotor angular velocity. J stands for the rotor moment of inertia, B is the friction coefficient, L_d and L_q present the d - q -axis stator inductors, n_p expresses the number of pole pairs, T_L is the load torque, Φ is the magnet flux linkage of inertia, R_s is the armature resistance.

Introducing variables as follows:

$$\begin{aligned}
 x_1 &= \theta, x_2 = \omega, x_3 = i_q, x_4 = i_d, \\
 a_1 &= \frac{3n_p\Phi}{2}, a_2 = \frac{3n_p(L_d - L_q)}{2}, \\
 b_1 &= -\frac{R_s}{L_q}, b_2 = -\frac{n_p L_d}{L_q}, b_3 = -\frac{n_p \Phi}{L_q}, b_4 = \frac{1}{L_q}, \\
 c_1 &= -\frac{R_s}{L_d}, c_2 = \frac{n_p L_q}{L_d}, c_3 = \frac{1}{L_d}.
 \end{aligned}
 \tag{2}$$

Then, PMSM system (1) is expressed by

$$\begin{aligned}
 \dot{x}_1 &= x_2 \\
 \dot{x}_2 &= -\frac{B}{J}x_2 + \frac{a_1}{J}x_3 + \frac{a_2}{J}x_3x_4 - \frac{T_L}{J} \\
 \dot{x}_3 &= b_3x_2 + b_1x_3 + b_2x_2x_4 + b_4u_q \\
 \dot{x}_4 &= c_1x_4 + c_2x_2x_3 + c_3u_d \\
 y &= x_1
 \end{aligned}
 \tag{3}$$

where y is the output.

Further, let $f_2(\bar{x}) = -\frac{B}{J}x_2 + (\frac{a_1}{J} - 1)x_3 + \frac{a_2}{J}x_3x_4 - \frac{T_L}{J}$, $f_3(\bar{x}) = b_3x_2 + b_1x_3 + b_2x_2x_4$ and $f_4(\bar{x}) = c_1x_4 + c_2x_2x_3$, $(\bar{x} = [x_1, x_2, x_3, x_4]^T)$.

Then system (3) becomes as follows

$$\begin{aligned}
 \dot{x}_1 &= x_2 \\
 \dot{x}_2 &= f_2(\bar{x}) + x_3 \\
 \dot{x}_3 &= f_3(\bar{x}) + b_4u_q \\
 \dot{x}_4 &= f_4(\bar{x}) + c_3u_d \\
 y &= x_1
 \end{aligned}
 \tag{4}$$

Assumption 1 [16]: Assume that all state variables in (3) are constrained in the compact sets $|x_i| < k_{c_i}$ and $k_{c_i} > 0$ are constants.

Assumption 2 [16]: There exist constants $Y_r > 0$ and $Y_0 > 0$ such that the desired trajectory y_r and \dot{y}_r satisfy $|y_r| \leq Y_r < k_{c_1}$ and $|\dot{y}_r| \leq k_r$.

Lemma 1 (Young’s Inequality): For any vectors $x, y \in R^n$, the following Young’s inequality holds:

$$x^T y \leq (\eta^\alpha / \alpha) \|x\|^\alpha + (1 / \eta^\beta) \|y\|^\beta$$

where $\eta > 0, \alpha > 1, \beta > 1$, and $(\alpha - 1)(\beta - 1) = 1$.

The control objectives of this study are to formulate an observer-based output feedback control scheme for PMSMs (4) by finite-time stability and neural networks, which ensure the controlled PMSM system to be stable and make the system output $y(t)$ track the referenced function $y_r(t)$ in finite time interval. Especially, all the state variables in the controlled PMSMs do not exceed the prescribed bounds.

2.2 Neural networks

According to [27] and [28], a radial basis function neural network is expressed as

$$\hat{f}(Z) = W^T S(Z) \tag{5}$$

where the input vector $Z \in R^p, W \in R^q$ is the weight vector with neurons number q . And $S(Z) = [S_1(Z), \dots, S_q(Z)]^T$, where $S_i(Z)$ are radial basis functions selected, which are chosen by

$$S_i(Z) = \exp\left(-\frac{(Z - \rho_i)^T (Z - \rho_i)}{\vartheta_i^2}\right), i = 1, \dots, q \tag{6}$$

In (6), $\rho_i = [\rho_{i,1}, \dots, \rho_{i,p}]^T$ are the centers and ϑ_i are the widths of the Gaussian function. The outstanding feature of a neural network $\hat{f}(Z) = W^T S(Z)$ is that it can approximate the smooth continuous function $f(Z)$, which is defined in a bounded closed set.

2.3 Finite-time stability theory

Definition 1 [19, 20]: Suppose $z = 0$ is the equilibrium point $\dot{z} = f(z)$. The nonlinear system $\dot{z} = f(z)$ is called to be semi-global practical finite-time stability (SGPFTS), if for any $z(t_0) = z_0$, there exist a $\varepsilon > 0$ and a settling time $T(\varepsilon, z_0) < \infty$, when $t \geq t_0 + T$, then $\|z(t)\| < \varepsilon$.

Lemma 2 [19, 20]: For the system $\dot{z} = f(z)$, if there exist a positive-definite function V , and positive constants $c > 0, 0 < \beta < 1$ and $D > 0$, and satisfying the following inequality:

$$\dot{V} \leq -cV^\beta + D, t \geq 0,$$

the system $\dot{z} = f(z)$ is called to be SGPFTS.

3 Finite-time adaptive output-feedback control design

In this section, we first give a neural state observer to estimate the immeasurable states of the PMSM system (4). Then an adaptive neural output feedback controller is developed by using the backstepping control design technique and the finite-time stability theory.

3.1 Neural state observer design

Note that since the friction coefficient B , the rotor moment of inertia J and the load torque T_L in PMSM system (4) are unknown, the functions $f_i(\bar{x})$ $i = 2, 3, 4$, are thus also unknown. In this situation, we use neural $\hat{f}_i(\bar{x}) = \hat{W}_i^T S_i(\bar{x})$ to approximate the unknown functions $f_i(\bar{x})$ and obtain an equivalent control design model for PMSM system (4). To begin with, we assume that

$$f_i(\bar{x}) = W_i^{*T} S_i(\bar{x}) + \varepsilon_i \tag{7}$$

where $i = 2, 3, 4$, W_i^* are ideal parameter vectors, ε_i are approximation errors, and $|\varepsilon_i| \leq \bar{\varepsilon}_i$, $\bar{\varepsilon}_i$ are known positive constants.

By (7), then PMSM system (4) is rewritten as

$$\begin{aligned} \dot{x}_1 &= x_2 \\ \dot{x}_2 &= x_3 + W_2^{*T} S_2(\bar{x}) + \varepsilon_2(\bar{x}) \\ \dot{x}_3 &= W_3^{*T} S_3(\bar{x}) + \varepsilon_3(\bar{x}) + b_4 u_q \\ \dot{x}_4 &= W_4^{*T} S_4(\bar{x}) + \varepsilon_4(\bar{x}) + c_3 u_d \end{aligned} \tag{8}$$

For the convenience of the following analysis, system (8) is rewritten in the following form:

$$\dot{x} = A_0 x + Ly + \sum_{i=2}^4 B_i W_i^{*T} S_i(\bar{x}) + \varepsilon(\bar{x}) + Ku \tag{9}$$

where $x = [x_1 \ x_2 \ x_3 \ x_4]^T$, $A_0 = \begin{bmatrix} -l_1 & 1 & 0 & 0 \\ -l_2 & 0 & 1 & 0 \\ -l_3 & 0 & 0 & 0 \\ -l_4 & 0 & 0 & 0 \end{bmatrix}$,

$L = [l_1 \ l_2 \ l_3 \ l_4]^T$, $B_2 = [0 \ 1 \ 0 \ 0]^T$, $B_3 = [0 \ 0 \ 1 \ 0]^T$, $B_4 = [0 \ 0 \ 0 \ 1]^T$,

$\varepsilon = [0 \ \varepsilon_2 \ \varepsilon_3 \ \varepsilon_4]^T$, $K = \begin{bmatrix} 0 & \dots & 0 \\ \vdots & b_4 & \vdots \\ 0 & \dots & c_3 \end{bmatrix}$,

$u = [0 \ 0 \ u_q \ u_d]^T$. To obtain the estimations of immeasurable states, a neural network state observer is designed as

$$\dot{\hat{x}} = A_0 \hat{x} + \sum_{i=2}^4 B_i \hat{W}_i^T S_i(\hat{x}) + Ku + Ly \tag{10}$$

where $= [\hat{x}_1 \ \hat{x}_2 \ \hat{x}_3 \ \hat{x}_4]^T$ and \hat{W}_i are estimates of $x = [x_1 \ x_2 \ x_3 \ x_4]^T$ and W_i^* , respectively.

In state observer (10), observer gains l_i ($i = 1, 2, 3, 4$) are selected such that matrix A_0 is a Hurwitz. Then there exists a positive definite matrix $P = P^T > 0$ satisfying

$$A_0^T P + PA_0 = -2Q \tag{11}$$

where $Q = Q^T > 0$ is a given positive definite matrix.

3.2 Finite-time adaptive neural control design

In this part, we give an adaptive neural controller by the backstepping control design technique and the finite-time theory.

The change of coordinates is first given as.

$$\begin{aligned} z_1 &= x_1 - y_r \\ z_2 &= \hat{x}_2 - \alpha_1 \\ z_3 &= \hat{x}_3 - \alpha_2 \end{aligned} \tag{12}$$

where y_r is the desired reference, α_1 and α_2 are the virtual controllers.

This specific finite-time output feedback control design process is as follows:

Step 1: The time derivative of z_1 along with (8) and (12) is

$$\begin{aligned} \dot{z}_1 &= \dot{x}_1 - \dot{y}_r \\ &= z_2 + e_2 + \alpha_1 - \dot{y}_r \end{aligned} \tag{13}$$

Construct the barrier Lyapunov function as follows:

$$V_1 = \frac{1}{2} \log \frac{k_{b_1}^2}{k_{b_1}^2 - z_1^2} \tag{14}$$

where $k_{b_1} > 0$, and the set $\Omega_{z_1} = \{z_1 : |z_1| < k_{b_1}\}$ is a compact set containing origin.

By the barrier Lyapunov function (14), we design the virtual controller as

$$\alpha_1 = -\frac{k_1 \text{sgn}(z_1) z_1^{2\beta-1}}{(k_{b_1}^2 - z_1^2)^{\beta-1}} - \frac{z_1}{2(k_{b_1}^2 - z_1^2)} + \dot{y}_r \tag{15}$$

where the designed parameters $k_1 > 0$ and $0 < \beta < 1$.

Step 2: By (8), the time derivative of $z_2 = \hat{x}_2 - \alpha_1$ is

$$\begin{aligned} \dot{z}_2 &= \dot{\hat{x}}_2 - \dot{\alpha}_1 \\ &= \hat{x}_3 + \hat{W}_2^T S_2 + l_2 e_1 - \dot{\alpha}_1 \\ &= z_3 + \alpha_2 + \hat{W}_2^T S_2 + l_2 e_1 - \dot{\alpha}_1 \end{aligned} \tag{16}$$

Construct the following barrier Lyapunov function candidate as:

$$V_2 = \frac{1}{2} \log \frac{k_{b_2}^2}{k_{b_2}^2 - z_2^2} + \frac{1}{2r_2} \tilde{W}_2^T \tilde{W}_2 \tag{17}$$

where $r_2 > 0$ is the design parameter, V_2 is continuous in the set $\Omega_{z_2} = \{z_2 : |z_2| < k_{b_2}\}$.

By using V_2 , we design the virtual controller α_2 and updating law of \hat{W}_2 as

$$\alpha_2 = -\frac{k_2 \text{sgn}(z_2) z_2^{2\beta-1}}{(k_{b_2}^2 - z_2^2)^{\beta-1}} - \frac{k_{b_2}^2 - z_2^2}{k_{b_1}^2 - z_1^2} z_1 - \frac{z_2}{2(k_{b_2}^2 - z_2^2)} - \hat{W}_2^T S_2 - l_2 e_1 + \dot{\alpha}_1$$
(18)

$$\dot{\hat{W}}_2 = -\sigma_2 \hat{W}_2 + \frac{r_2 z_2}{k_{b_2}^2 - z_2^2} S_2$$
(19)

where $k_2 > 0$ and $\sigma_2 > 0$ are designed parameters.

Step 3: By (8) and $z_3 = \hat{x}_3 - \alpha_2$, we have the time derivative of z_3 ,

$$\begin{aligned} \dot{z}_3 &= \dot{\hat{x}}_3 - \dot{\alpha}_2 \\ &= \hat{W}_3^T S_3 + b_4 u_q + l_3 e_1 - \dot{\alpha}_2 \end{aligned}$$
(20)

Select the following barrier Lyapunov function candidate as:

$$V_3 = \frac{1}{2} \log \frac{k_{b_3}^2}{k_{b_3}^2 - z_3^2} + \frac{1}{2r_3} \tilde{W}_3^T \tilde{W}_3$$
(21)

where $r_3 > 0$ is the design parameter, V_3 is continuous in the set $\Omega_{z_3} = \{z_3 : |z_3| < k_{b_3}\}$.

Similar to step 2, the actual controller u_q and updating law of \hat{W}_3 are designed by

$$u_q = \frac{1}{b_4} \left[-\frac{k_3 \text{sgn}(z_3) z_3^{2\beta-1}}{(k_{b_3}^2 - z_3^2)^{\beta-1}} - \frac{k_{b_3}^2 - z_3^2}{k_{b_2}^2 - z_2^2} z_2 - \hat{W}_3^T S_3 - \frac{z_3}{2(k_{b_3}^2 - z_3^2)} - l_3 e_1 + \dot{\alpha}_2 \right]$$
(22)

$$\dot{\hat{W}}_3 = -\sigma_3 \hat{W}_3 + \frac{r_3 z_3}{k_{b_3}^2 - z_3^2} S_3$$
(23)

where $k_3 > 0$ and $\sigma_3 > 0$ are designed parameters.

Step 4: By (8) and define $z_4 = \hat{x}_4$, we have

$$\dot{z}_4 = \dot{\hat{x}}_4 = \hat{W}_4^T S_4 + c_3 u_d + l_4 e_1$$
(24)

Select the following barrier Lyapunov function candidate as:

$$V_4 = \frac{1}{2} \log \frac{k_{b_4}^2}{k_{b_4}^2 - z_4^2} + \frac{1}{r_4} \tilde{W}_4^T \tilde{W}_4$$
(25)

where $r_4 > 0$ is the design parameter, V_4 is continuous in the set $\Omega_{z_4} = \{z_4 : |z_4| < k_{b_4}\}$. Based on the barrier Lyapunov function (25), we design the actual controller u_d and updating law of \hat{W}_4 as follows

$$u_d = \frac{1}{c_3} \left[-\frac{k_4 \text{sgn}(z_4) z_4^{2\beta-1}}{(k_{b_4}^2 - z_4^2)^{\beta-1}} - \frac{z_4}{2(k_{b_4}^2 - z_4^2)} - \hat{W}_4^T S_4 - l_4 e_1 \right]$$
(26)

$$\dot{\hat{W}}_4 = -\sigma_4 \hat{W}_4 + \frac{r_4 z_4}{k_{b_4}^2 - z_4^2} S_4$$
(27)

where $k_4 > 0$ and $\sigma_4 > 0$ are designed parameters.

The configuration of the above designed neural adaptive output-feedback controllers is displayed in Fig. 2.

3.3 Stability analysis

The main merits of the proposed controllers in the above sections are as follows:

Theorem 1 For the PMSM system (1) under the Assumption 1 and Assumption 2, if we adopt adaptive control scheme consisting of the virtual controllers (15), (18), the actual controllers (22), (26), neural network adaptive state observer (9), and parameter updating laws (19), (23) and (27), then the following properties are guaranteed

- (i) All the closed-loop system signals are boundedness;

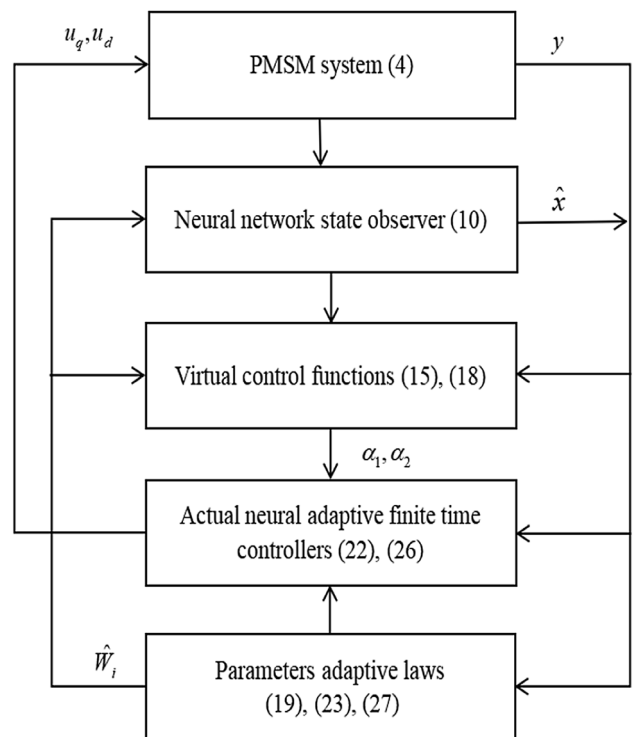


Fig. 2 Finite-time neural network adaptive output feedback backstepping control scheme

- (ii) The observer errors and tracking errors converge in a finite-time interval;
- (iii) All the state variables do not exceed their prescribed bounds.

Proof Define the observer errors as $e_i = x_i - \hat{x}_i (i = 1, 2, 3, 4)$, then from (9) and (10), we have the error dynamics equation:

$$\dot{e} = A_0 e + \sum_{i=2}^4 B_i [W_i^{*T} (S_i(\bar{x}) - S_i(\hat{x})) + \tilde{W}_i^T S_i(\hat{x})] + \varepsilon(\bar{x}) \tag{28}$$

where $e = [e_1 \ e_2 \ e_3 \ e_4]^T$, $\tilde{W}_i = W_i^* - \hat{W}_i (i = 2, 3, 4)$.

Choose the Lyapunov function

$$V_0 = \frac{1}{2} e^T P e \tag{29}$$

By (28), we have \dot{V}_0 as

$$\begin{aligned} \dot{V}_0 &= \frac{1}{2} (\dot{e}^T P e + e^T P \dot{e}) \\ &= -e^T Q e + e^T P \varepsilon + e^T P \sum_{i=2}^4 B_i \tilde{W}_i^T S_i(\hat{x}) \\ &\quad + e^T P \sum_{i=2}^4 B_i W_i^{*T} (S_i(\bar{x}) - S_i(\hat{x})) \end{aligned} \tag{30}$$

By using the Young’s inequality, we obtain

$$e^T P \varepsilon \leq \frac{1}{2} \|e\|^2 + \frac{1}{2} \|P\|^2 \|\bar{\varepsilon}\|^2 \tag{31}$$

$$e^T P \sum_{i=2}^4 B_i \tilde{W}_i^T S_i(\hat{x}) \leq \frac{1}{2} \|e\|^2 + \frac{1}{2} \|P\|^2 \sum_{i=2}^4 \tilde{W}_i^T \tilde{W}_i \tag{32}$$

$$e^T P \sum_{i=2}^4 B_i W_i^{*T} (S_i(\bar{x}) - S_i(\hat{x})) \leq \|e\|^2 + \|P\|^2 \sum_{i=2}^4 \|W_i^*\|^2 \tag{33}$$

Substituting (31)–(33) into (30), we obtain

$$\begin{aligned} \dot{V}_0 &\leq -e^T Q e + 2\|e\|^2 + \|P\|^2 \\ &\quad \left(\sum_{i=2}^4 \left(\frac{1}{2} \tilde{W}_i^T \tilde{W}_i + \|W_i^*\|^2 \right) + \frac{1}{2} \|\bar{\varepsilon}\|^2 \right) \\ &\leq -\lambda_0 \|e\|^2 + \frac{1}{2} \|P\|^2 \sum_{i=2}^4 \tilde{W}_i^T \tilde{W}_i + D_0 \end{aligned} \tag{34}$$

where $\lambda_0 = (\lambda_{\min}(Q) - 2) > 0$, $\lambda_{\min}(Q)$ denotes the minimum eigenvalue of matrix Q .

$$D_0 = \frac{1}{2} \|P\|^2 \|\bar{\varepsilon}\|^2 + \|P\|^2 \sum_{i=2}^4 \|W_i^*\|^2.$$

Choose the whole Lyapunov function as follows

$$\begin{aligned} V &= V_0 + \sum_{i=1}^4 V_i \\ &= \frac{1}{2} e^T P e + \frac{1}{2} \sum_{i=1}^4 \log \frac{k_{b_i}^2}{k_{b_i}^2 - z_i^2} + \sum_{i=2}^4 \frac{1}{2r_i} \tilde{W}_i^T \tilde{W}_i \end{aligned} \tag{35}$$

From (34) and (35), \dot{V} is as follows

$$\begin{aligned} \dot{V} &= \dot{V}_0 + \sum_{i=1}^4 \dot{V}_i \\ &\leq -\lambda_0 \|e\|^2 + \frac{1}{2} \|P\|^2 \sum_{i=2}^4 \tilde{W}_i^T \tilde{W}_i + D_0 \\ &\quad + \sum_{i=1}^4 \frac{z_i \dot{z}_i}{k_{b_i}^2 - z_i^2} - \sum_{i=2}^4 \frac{1}{r_i} \tilde{W}_i^T \dot{\tilde{W}}_i \end{aligned} \tag{36}$$

Substituting (13), (16), (20), (24) into (36) yields

$$\begin{aligned} \dot{V} &\leq -\lambda_0 \|e\|^2 + \frac{1}{2} \|P\|^2 \sum_{i=2}^4 \tilde{W}_i^T \tilde{W}_i + D_0 \\ &\quad + \sum_{i=1}^4 \frac{z_i}{k_{b_i}^2 - z_i^2} \tau_i - \sum_{i=2}^4 \frac{1}{r_i} \tilde{W}_i^T \left(\dot{\tilde{W}}_i - \frac{r_i z_i}{k_{b_i}^2 - z_i^2} S_i \right) \end{aligned} \tag{37}$$

In (37), $\tau_1 = z_2 + \alpha_1 + e_2 - \dot{y}_r$, $\tau_2 = z_3 + \alpha_2 + \hat{W}_2^T S_2 - \tilde{W}_2^T S_2 + l_2 e_1 - \dot{\alpha}_1$, $\tau_3 = \hat{W}_3^T S_3 - \tilde{W}_3^T S_3 + u_q + l_3 e_1 - \dot{\alpha}_2$, $\tau_4 = \hat{W}_4^T S_4 - \tilde{W}_4^T S_4 + u_d + l_4 e_1$.

By using the Young’s inequality, we obtain

$$\frac{z_1 e_2}{k_{b_1}^2 - z_1^2} \leq \frac{z_1^2}{2(k_{b_1}^2 - z_1^2)^2} + \frac{1}{2} \|e\|^2 \tag{38}$$

$$-\frac{z_i}{k_{b_i}^2 - z_i^2} \tilde{W}_i^T S_i \leq \frac{z_i^2}{2(k_{b_i}^2 - z_i^2)^2} + \frac{1}{2} \tilde{W}_i^T \tilde{W}_i, \quad i = 2, 3, 4 \tag{39}$$

Substituting (38)–(39) into (37) yields

$$\begin{aligned} \dot{V} &\leq -\lambda \|e\|^2 + \frac{1}{2} \|P\|^2 \sum_{i=2}^4 \tilde{W}_i^T \tilde{W}_i + D_0 \\ &\quad - \sum_{i=2}^4 \frac{1}{r_i} \tilde{W}_i^T \left(\dot{\tilde{W}}_i - \frac{r_i z_i}{k_{b_i}^2 - z_i^2} S_i \right) \\ &\quad + \frac{1}{2} \sum_{i=2}^4 \tilde{W}_i^T \tilde{W}_i + \sum_{i=1}^4 \frac{z_i}{k_{b_i}^2 - z_i^2} \kappa_i \end{aligned} \tag{40}$$

where $\lambda = \lambda_0 + 1$, $\kappa_1 = \frac{z_1}{2(k_{b_1}^2 - z_1^2)} + z_2 + \alpha_1 - \dot{y}_r$, $\kappa_2 = \frac{z_2}{2(k_{b_2}^2 - z_2^2)} + z_3 + \alpha_2 + \hat{W}_2^T S_2 + l_2 e_1 - \dot{\alpha}_1$, $\kappa_3 = \frac{z_3}{2(k_{b_3}^2 - z_3^2)} + \hat{W}_3^T S_3 + u_q + l_3 e_1 - \dot{\alpha}_2$, $\kappa_4 = \frac{z_4}{2(k_{b_4}^2 - z_4^2)} + \hat{W}_4^T S_4 + u_d + l_4 e_1$.

By substituting the controllers (15), (18), (22) and (26) into (40), and using the parameter updating laws (19), (23) and (27), then (40) becomes

$$\begin{aligned} \dot{V} \leq & -\lambda \|e\|^2 + \frac{1}{2} \|P\|^2 \sum_{i=2}^4 \tilde{W}_i^T \tilde{W}_i + D_0 \\ & - \sum_{i=1}^4 \frac{k_i z_i^{2\beta}}{(k_{b_i}^2 - z_i^2)^\beta} + \sum_{i=2}^4 \left(\frac{\sigma_i}{r_i} \tilde{W}_i^T \tilde{W}_i + \frac{1}{2} \tilde{W}_i^T \tilde{W}_i \right) \end{aligned} \tag{41}$$

Note that the following inequality holds

$$\frac{\sigma_i}{r_i} \tilde{W}_i^T \tilde{W}_i \leq -\frac{\sigma_i}{2r_i} \tilde{W}_i^T \tilde{W}_i + \frac{\sigma_i}{2r_i} \|W_i^*\|^2, \quad i = 2, 3, 4 \tag{42}$$

Thus, from inequality (42), (41) can be rewritten as

$$\begin{aligned} \dot{V} \leq & -\lambda \|e\|^2 - \frac{1}{2} \sum_{i=2}^4 \left(\frac{\sigma_i}{r_i} - \|P\|^2 - 1 \right) \tilde{W}_i^T \tilde{W}_i \\ & - \sum_{i=1}^4 \frac{k_i z_i^{2\beta}}{(k_{b_i}^2 - z_i^2)^\beta} + \bar{D} \end{aligned} \tag{43}$$

where $\bar{D} = D_0 + \sum_{i=2}^4 \frac{\sigma_i}{2r_i} \|W_i^*\|^2$.

Let $\delta = \min\{2^\beta k_1, 2^\beta k_i, \frac{\sigma_i}{r_i} - \|P\|^2 - 1, i = 2, 3, 4\}$, then (43) can be expressed by

$$\begin{aligned} \dot{V} \leq & -\frac{2\lambda}{\lambda_{\max}(P)} \frac{1}{2} e^T P e \\ & - \delta \left\{ \sum_{i=1}^4 \left(\frac{z_i^2}{2(k_{b_i}^2 - z_i^2)} \right)^\beta - \sum_{i=2}^4 \frac{1}{2} \tilde{W}_i^T \tilde{W}_i \right\} + \bar{D} \end{aligned} \tag{44}$$

By using the following inequality

$$|\Theta|^v |\Psi|^m \leq \frac{v}{v+m} n |\Theta|^{v+m} + \frac{m}{v+m} n^{-\frac{v}{m}} |\Psi|^{v+m}$$

and selecting $\varphi = 1$, $\phi = 1 - \beta$, $v = \beta$ and $\tau = \beta^{(\beta/1-\beta)}$, then, we can obtain

$$\left(\frac{1}{2} e^T P e \right)^\beta \leq (1 - \beta)\tau + \frac{1}{2} e^T P e \tag{45}$$

$$\left(\sum_{i=2}^4 \frac{1}{2} \tilde{W}_i^T \tilde{W}_i \right)^\beta \leq (1 - \beta)\tau + \sum_{i=2}^4 \frac{1}{2} \tilde{W}_i^T \tilde{W}_i \tag{46}$$

Note that $\log(k_{b_i}^2 / (k_{b_i}^2 - z_i^2)) \leq (z_i^2 / (k_{b_i}^2 - z_i^2))$, when $|z_i| < k_{b_i}$. Substituting (45)–(46) into (44) gives

$$\begin{aligned} \dot{V} \leq & -\frac{2\lambda}{\lambda_{\max}(P)} \left(\frac{1}{2} e^T P e \right)^\beta - \delta \sum_{i=1}^4 \left(\frac{1}{2} \log \frac{k_{b_i}^2}{k_{b_i}^2 - z_i^2} \right)^\beta \\ & - \delta \left(\sum_{i=2}^4 \frac{1}{2} \tilde{W}_i^T \tilde{W}_i \right)^\beta + D \end{aligned} \tag{47}$$

where $D = \bar{D} + 2\delta\tau(1 - \beta) + (2\lambda/\lambda_{\max}(P))(1 - \beta)\tau$.

Define $c = \min\{\lambda 2^\beta / \lambda_{\max}(P), \delta\}$, then we can obtain

$$V \leq -cV^\beta + D \tag{48}$$

By the inequality (48), we follow that the closed-loop system is SGPFSS.

Further, based on (48), the following inequality holds

$$V \leq \left[\frac{D}{(1 - \gamma)c} \right]^\frac{1}{\beta}, t \geq T_0 \tag{49}$$

where $T_0 = \frac{V^{1-\beta}(0)}{c(1-\beta)(1-\gamma)}$, $0 < \gamma < 1$.

From (35) and (49), $\forall t \geq T_0$, we have that $|y - y_r| \leq k_{b1} [1 - e^{-2(\frac{D}{(1-\gamma)c})^{-\beta}}]^\frac{1}{2} < k_{b1}$, which means that tracking error is bonded by k_{b1} . Moreover, it can be made to be smaller after the settling time T_0 and by adjusting the parameters appropriately.

With the above derivations, we easily derive that $|x_1| \leq |z_1| + |y_r| < k_{b1} + Y_r$. By selecting $k_{b1} = k_{c1} - Y_r$, we can obtain $|x_1| < k_{c1}$. Obviously, α_1 is bounded and $|\alpha_1| < \bar{\alpha}_1$. And $x_2 = z_2 + \alpha_1$. Therefore, $|x_2| \leq |z_2| + |\alpha_1| < k_{c2}$ is true, which means $|x_2| < k_{c2}$. Similarly, we have proved that $|x_3| < k_{c3}$ and $|x_4| < k_{c4}$. \square

4 Simulation study

In this part, the computer simulation and the comparison with the previous control method are carried out by MATLAB software to demonstrate the effectiveness of the developed control method. The parameters in the considered PMSMs (4) are listed by Table 1 [15].

The referenced function is given as $y_r = \sin(t + 0.1)$. As the same in [16], the state variables are restricted by $|x_1| < 2.5$, $|x_2| < 50$, $|x_3| < 25$, $|x_4| < 25$.

We design the neural networks $\hat{f}_i(\bar{x}) = \hat{W}_i^T S_i(\bar{x})$ to approximate the functions $f_i(\bar{x})$ in PMSMs (4). Each neural network contains five nodes and radial basis functions are chosen by $S_i(x) = \exp(-\frac{(x-\rho_i)^T(x-\rho_i)}{\vartheta_i^2})$, where

Table 1 The parameters of the considered PMSMs

Parameter	Value	Unit
Rotor moment of inertia	0.0086	kg · m ²
Friction coefficient	0.00217	N · M/(rad/s)
Magnet flux linkage of inertia	0.7	Wb
q-axis stator inductor	0.058	H
d-axis stator inductor	0.00285	H
Number of pole pairs	4	
Armature resistance	0.046	Ω

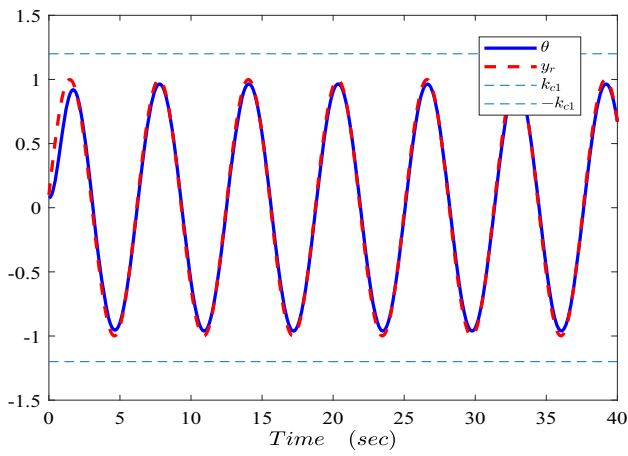


Fig. 3 The trajectories of the rotor position θ with reference signal y_r

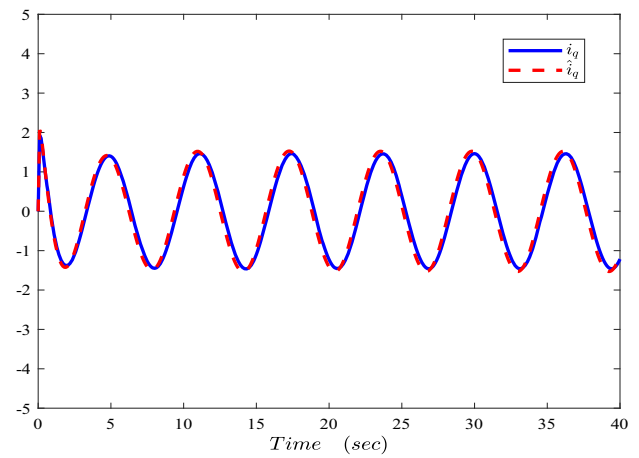


Fig. 6 The trajectories of the current i_q and its estimate \hat{i}_q

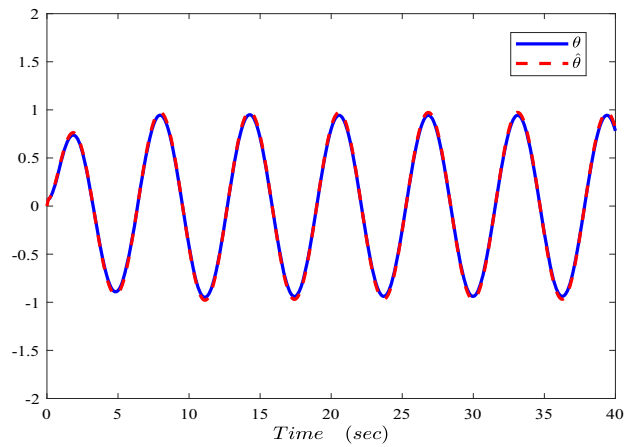


Fig. 4 The trajectories of the rotor position θ and its estimate $\hat{\theta}$

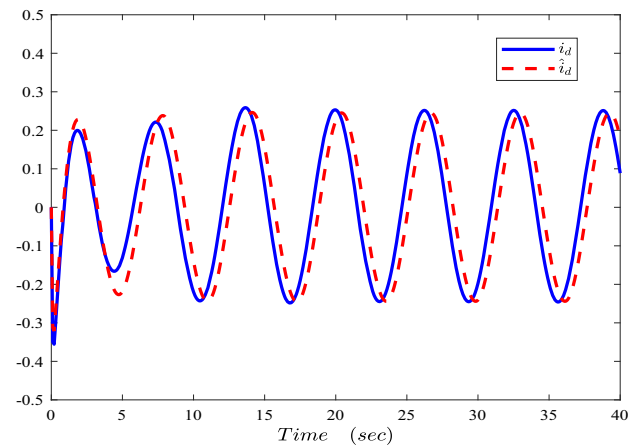


Fig. 7 The trajectories of the current i_d and its estimate \hat{i}_d

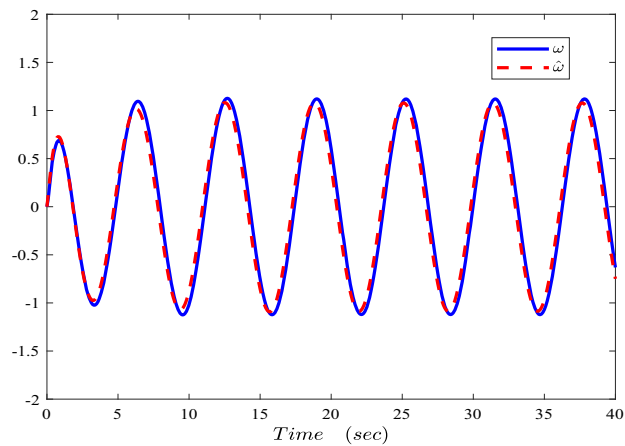


Fig. 5 The trajectories of angular velocity ω and its estimate $\hat{\omega}$

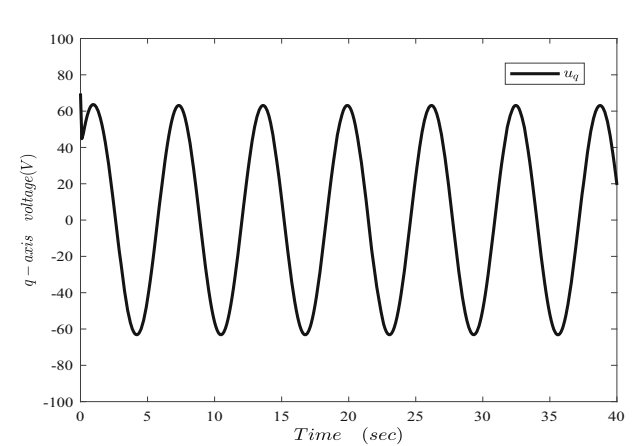


Fig. 8 The trajectory of the voltage u_q

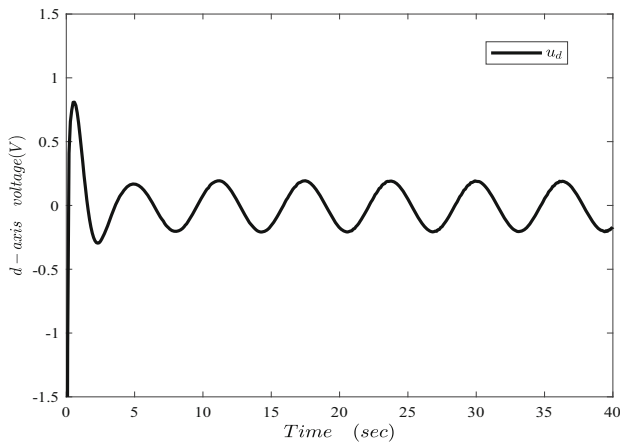


Fig. 9 The trajectory of the voltage u_d

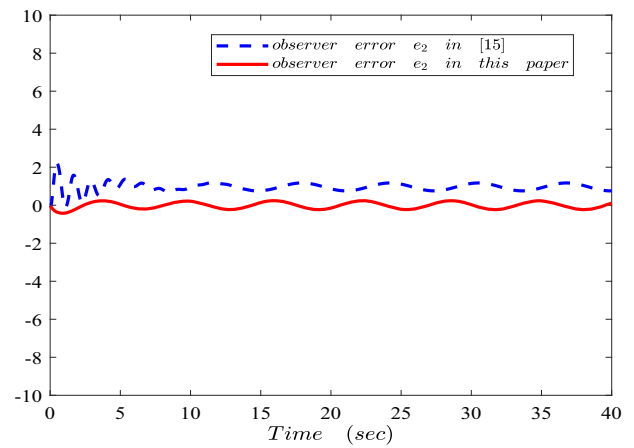


Fig. 12 The observer errors e_2

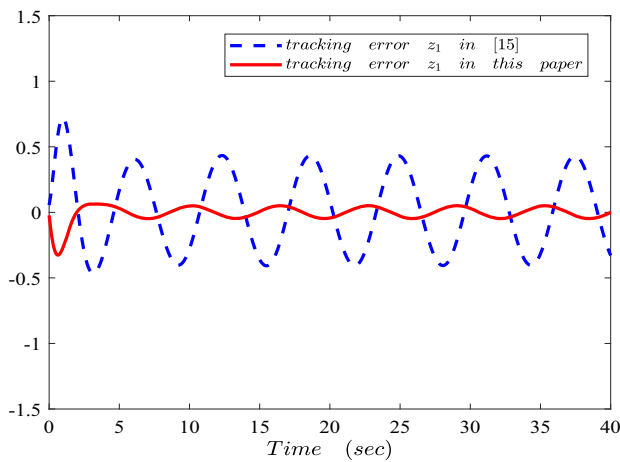


Fig. 10 The tracking errors of z_1

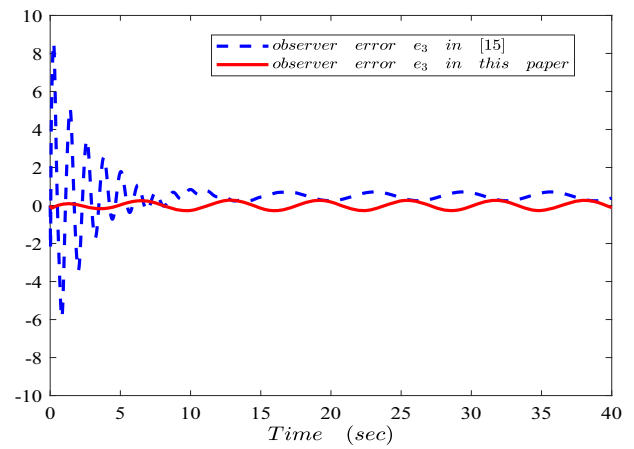


Fig. 13 The observer errors e_3

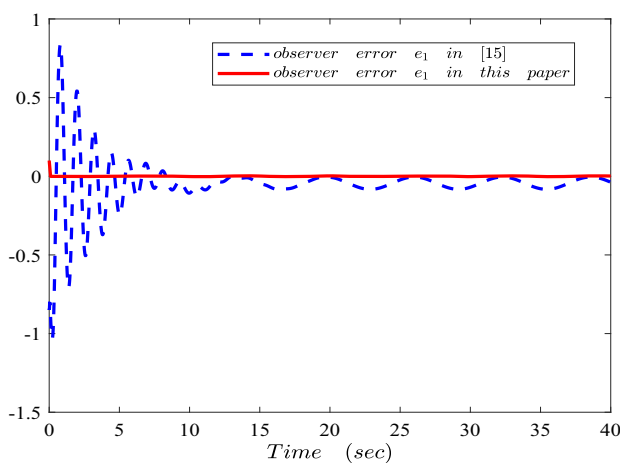


Fig. 11 The observer errors e_1

$\rho_{ij} = [j - 2, j - 2]^T$, $i = 2, 3, 4$, $j = 1, 2, 3, 4, 5$, and variance $\vartheta_i = 4$.

The neural adaptive state observers are designed as

$$\begin{aligned}
 \dot{\hat{x}}_1 &= \hat{x}_2 + l_1(y - \hat{x}_1) \\
 \dot{\hat{x}}_2 &= \hat{x}_3 + \hat{W}_2^T S_2(\hat{x}) + l_2(y - \hat{x}_1) \\
 \dot{\hat{x}}_3 &= \hat{W}_3^T S_3(\hat{x}) + b_4 u_q + l_3(y - \hat{x}_1) \\
 \dot{\hat{x}}_4 &= \hat{W}_4^T S_4(\hat{x}) + c_3 u_d + l_4(y - \hat{x}_1)
 \end{aligned} \tag{50}$$

The observer gain vector L is selected as $L = [l_1, l_2, l_3, l_4]^T = [1, 50, 250, 20]^T$ and A is a Hurwitz matrix. Then, given a definite matrix $Q = I$, by solving Lyapunov equation $A_0^T P + P A_0 = -2I$, we obtain

$$P = \begin{bmatrix} 0.1629 & 0.8371 & 0.081 & 0.05 \\ 0.8371 & 9.0629 & 40.8552 & 3.3079 \\ 0.0810 & 40.8552 & 210.0163 & 19.2421 \\ 0.05 & 3.3079 & 19.2421 & 14.1194 \end{bmatrix}$$

The virtual controllers and the actual controllers are as follows

$$\alpha_1 = -\frac{k_1 \operatorname{sgn}(z_1) z_1^{2\beta-1}}{(k_{b_1}^2 - z_1^2)^{\beta-1}} - \frac{z_1}{2(k_{b_1}^2 - z_1^2)} + \dot{y}_r \tag{51}$$

$$\alpha_2 = -\frac{k_2 \operatorname{sgn}(z_2) z_2^{2\beta-1}}{(k_{b_2}^2 - z_2^2)^{\beta-1}} - \frac{k_{b_2}^2 - z_2^2}{k_{b_1}^2 - z_1^2} z_1 - \frac{z_2}{2(k_{b_2}^2 - z_2^2)} - \hat{W}_2^T S_2 - l_2 e_1 + \dot{\alpha}_1 \tag{52}$$

$$u_q = \frac{1}{b_4} \left[-\frac{k_3 \operatorname{sgn}(z_3) z_3^{2\beta-1}}{(k_{b_3}^2 - z_3^2)^{\beta-1}} - \frac{k_{b_3}^2 - z_3^2}{k_{b_2}^2 - z_2^2} z_2 - \hat{W}_3^T S_3 - \frac{z_3}{2(k_{b_3}^2 - z_3^2)} - l_3 e_1 + \dot{\alpha}_2 \right] \tag{53}$$

$$u_d = \frac{1}{c_3} \left[-\frac{k_4 \operatorname{sgn}(z_4) z_4^{2\beta-1}}{(k_{b_4}^2 - z_4^2)^{\beta-1}} - \frac{z_4}{2(k_{b_4}^2 - z_4^2)} - \hat{W}_4^T S_4 - l_4 e_1 \right] \tag{54}$$

And also, the parameter updating laws are given as

$$\dot{\hat{W}}_i = -\sigma_i \hat{W}_i + \frac{r_i z_i}{k_{b_i}^2 - z_i^2} S_i, \quad i = 2, 3, 4 \tag{55}$$

The design parameters in (51)–(55) are chosen as: $k_1 = 20$, $k_2 = 25$, $k_3 = 30$, $k_4 = 50$; $k_{b_i} = 1.5$, ($i = 1, 3, 4$), $r_i = 0.01$, ($i = 2, 3, 4$); $\sigma_i = 20$, ($i = 2, 3, 4$); $\beta = 0.99$. Setting $x_1(0) = 0.1$, $x_2(0) = 0.01 \text{ rad/s}$, and $x_3(0) = 0.01 \text{ A}$, and other initial values are zeros.

The closed-loop responses are depicted in Figs. 3, 4, 5, 6, 7, 8, 9. Figure. 3 is the responses of rotor position θ and reference signal y_r . Figures 4, 5, 6, 7 are the trajectories of rotor position θ , the angular velocity ω , the current i_q and the current i_d and their estimates $\hat{\theta}$, $\hat{\omega}$, \hat{i}_q and \hat{i}_d , respectively.

From Figs. 3, 4, 5, 6, 7, 8, 9, it is clearly that the control method of this paper can guarantee that the PMSMs is stable, its stator current and angular velocity do not exceed

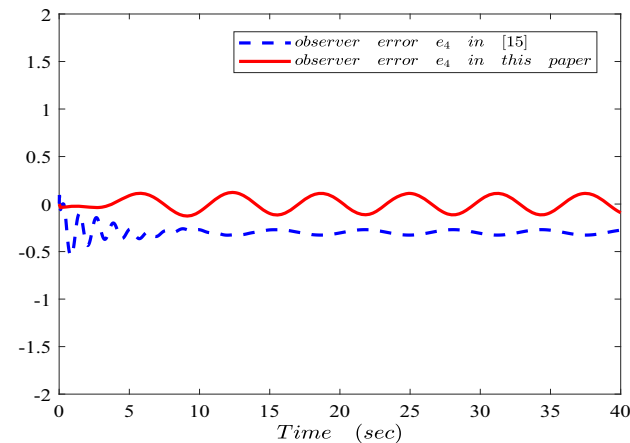


Fig. 14 The observer errors e_4

their predefined bounds. Furthermore, the tracking and observer errors converge in a finite-time.

To further demonstrate the effectiveness of the formulated controller in this study, we make a simulation comparison with the adaptive controller method in [15] designed based on asymptotic stability theory. In the simulation, the initial conditions of the variables and the updating parameters are selected as the same as the above simulation. Figures 10, 11, 12, 13, 14 give the trajectories of the tracking error z_1 and observer errors e_i .

Figures 10, 11, 12, 13 and 14 indicate that tracking and observer errors in this paper converge in a shorter time than those in [15]. Besides, the control performances are also better than [15].

5 Conclusion

In this paper, an adaptive neural network finite-time output-feedback control scheme is proposed for the PMSMs with unknown nonlinear functions and unmeasured constraint states. The neural networks are exploited to approximate the unknown nonlinear dynamics. By designing an adaptive neural state observer, the finite-time adaptive neural control method has been developed by constructing barrier Lyapunov functions. The main advantages of the presented finite-time adaptive neural control scheme ensure that the controlled PMSM system is SGPFTS and the tracking error converge to a small neighborhood of zero in a finite time. Furthermore, all the states of the control system do not exceed the given bounds. Computer simulation and comparison results have proved the effectiveness of the proposed control method. The further study direction will focus on the neural network event-triggered output feedback control for PMSMs based on this study.

Acknowledgements This work is supported in part by the National Natural Science Foundation of China (under Grant Nos. 62173172 and U22A2043) and in part by the Key Laboratory of Intelligent Manufacturing Technology (Shantou University), Ministry of Education (under grant No. 202109244).

Data Availability Data sharing is not applicable to this article as no datasets were generated or analysed during the current study.

Declarations

Conflict of interest The authors declared that they have no conflicts of interest to this work.

References

1. Chaoui H, Khayamy M, Okoye O (2018) Adaptive RBF network based direct voltage control for interior PMSM based vehicles. *IEEE Trans Veh Technol* 67(7):5740–5749

2. Dai Y, Ni S, Xu D (2021) Disturbance-observer based prescribed-performance fuzzy sliding mode control for PMSM in electric vehicles. *Eng Appl Artif Intell* 104:104361
3. Fung RF, Kung YS, Wu GC (2010) Dynamic analysis and system identification of an LCD glass-handling robot driven by a PMSM. *Appl Math Model* 34(5):1360–1381
4. Yuan T, Wang D, Wang X (2019) High-precision servo control of industrial robot driven by PMSM-DTC utilizing composite active vectors. *IEEE Access* 7:7577–7587
5. Zhou J, Wang Y (2002) Adaptive backstepping speed controller design for a permanent magnet synchronous motor. *IEE Pro-Elec Power Appl* 149(2):165–172
6. Morawiec M (2013) The adaptive backstepping control of permanent magnet synchronous motor supplied by current source inverter. *IEEE Trans Industr Inf* 9(2):1047–1055
7. Liu J, Li H, Deng Y (2017) Torque ripple minimization of PMSM based on robust ILC via adaptive sliding mode control. *IEEE Trans Power Electron* 33(4):3655–3671
8. Chaoui H, Sicard P (2011) Adaptive Lyapunov-based neural network sensorless control of permanent magnet synchronous machines. *Neural Comput Appl* 20(5):717–727
9. Deniz E (2017) ANN-based MPPT algorithm for solar PMSM drive system fed by direct-connected PV array. *Neural Comput Appl* 28(10):3061–3072
10. Yu J, Ma Y, Chen B (2011) Adaptive fuzzy backstepping position tracking control for a permanent magnet synchronous motor. *Int J Innov Comput Inform Control* 7(4):1589–1602
11. Li S, Gu H (2012) Fuzzy adaptive internal model control schemes for PMSM speed-regulation system. *IEEE Trans Industr Inf* 8(4):767–779
12. Mao W, Liu G (2019) Development of an adaptive fuzzy sliding mode trajectory control strategy for two-axis PMSM-driven stage application. *Int J Fuzzy Syst* 21(3):793–808
13. Gao J, Shi L, Deng L (2017) Finite-time adaptive chaos control for permanent magnet synchronous motor. *J Comput Appl* 37(2):597–601
14. Wang XJ, Wang SP (2016) Adaptive fuzzy robust control of PMSM with smooth inverse based dead-zone compensation. *Int J Control Autom Syst* 14(2):378–388
15. Chang W, Tong S (2017) Adaptive fuzzy tracking control design for permanent magnet synchronous motors with output constraint. *Nonlinear Dyn* 87(1):291–302
16. Liu Y, Yu J, Yu H, Lin C, Zhao L (2017) Barrier Lyapunov functions based adaptive neural control for permanent magnet synchronous motors with full state constraints. *IEEE Access* 5:10382–10389
17. Sakthivel R, Santra S, Kaviarasan B (2016) Finite-time sampled-data control of permanent magnet synchronous motor systems. *Nonlinear Dyn* 86(3):2081–2092
18. Yu J, Shi P, Dong W, Chen B, Lin C (2014) Neural network-based adaptive dynamic surface control for permanent magnet synchronous motors. *IEEE Trans Neural Networks Learn Syst* 26(3):640–645
19. Yang X, Yu J, Wang Q, Zhao L, Yu H, Lin C (2019) Adaptive fuzzy finite-time command filtered tracking control for permanent magnet synchronous motors. *Neurocomputing* 337(14):110–119
20. Lu S, Wang X, Wang L (2020) Finite-time adaptive neural network control for fractional-order chaotic PMSM via command filtered backstepping. *Adv Difference Equ* 1:1–21
21. Sun Y, Wu X, Bai L, Wei Z, Sun G (2016) Finite-time synchronization control and parameter identification of uncertain permanent magnet synchronous motor. *Neurocomputing* 207:511–518
22. Chen Q, Ren X, Na J (2017) Adaptive robust finite-time neural control of uncertain PMSM servo system with nonlinear dead zone. *Neural Comput Appl* 28(12):3725–3736
23. Lee H, Lee J (2012) Design of iterative sliding mode observer for sensorless PMSM control. *IEEE Trans Control Syst Technol* 21(4):1394–1399
24. Wang H, Li S, Lan Q (2017) Continuous terminal sliding mode control with extended state observer for PMSM speed regulation system. *Trans Inst Meas Control* 39(8):1195–1204
25. Zhao Y, Liu X, Zhang Q (2019) Predictive speed-control algorithm based on a novel extended-state observer for PMSM drives. *Appl Sci* 9(12):2575
26. Li S, Liu H, Ding S (2010) A speed control for a PMSM using finite-time feedback control and disturbance compensation. *Trans Inst Meas Control* 32(2):170–187
27. Wang T, Tong S, Li Y (2013) Adaptive neural network output feedback control of stochastic nonlinear systems with dynamical uncertainties. *Neural Comput Appl* 23(5):1481–1494
28. Tang L, Liu Y, Tong S (2014) Adaptive neural control using reinforcement learning for a class of robot manipulator. *Neural Comput Appl* 25(1):135–141

Publisher's Note Springer Nature remains neutral with regard to jurisdictional claims in published maps and institutional affiliations.

Springer Nature or its licensor (e.g. a society or other partner) holds exclusive rights to this article under a publishing agreement with the author(s) or other rightsholder(s); author self-archiving of the accepted manuscript version of this article is solely governed by the terms of such publishing agreement and applicable law.